INVITED PAPER

A CONTACTLESS MINORITY LIFETIME PROBE OF HETEROSTRUCTURES, SURFACES, INTERFACES AND BULK WAFERS

E. YABLONOVITCH and T. J. GMITTER

Bell Communications Research, Navesink Research Center, P.O. Box 7040, Red Bank, NJ 07701-7040, U.S.A.

Abstract—This paper reviews a contactless laser-pumped minority carrier lifetime probe which is of general utility in solid-state and semiconductor material measurements. This inductively coupled radio frequency probe has been used in a diverse array of measurements. It can study *minority* carrier properties, for example: epitaxial heterostructure quality comparing different growth methods; wafer substrate quality; interfacial recombination; chemical synthesis of nearly ideal electronic surfaces; and radiative electron–hole recombination. Correspondingly, *majority* carrier properties may also be probed: sheet conductivity of *p*-ZnSe layers for which ohmic contacts are unavailable; and band-bending at semiconductor surfaces in darkness and light. Most generally this transient radio frequency bridge is useful for rapid contactless monitoring of semiconductor process development.

INTRODUCTION

The goal of semiconductor research and development is generally to create an electrical component or device. Currents or voltages are applied through metal contacts. Contact metallurgy is often the most tedious and time-consuming part of semiconductor research.

While ohmic contacts are needed in the final device, they are frequently unnecessary for diagnostic measurements in the intermediate stages of device research and development. It is much faster to analyse the electrical performance of devices and materials by contactless, radio frequency induction without the need for ohmic contacts. That is, the electrical currents can be induced by magnetic induction from a radio frequency coil. At the same time, electrical carriers can be created by optical injection. In effect, both currents and voltages are created in a semiconductor wafer by a combination of radio and optical waves. In the development cycle, this cuts out the tedious clean-room processes which are required for the application of metal contacts. It allows rapid contactless evaluation of each stage of a fabrication cycle, permitting the discovery of defective processing steps in the sequence. We have been employing this approach since 1984, and it has rewarded us with a number of meaningful[1] discoveries in the semiconductor materials field.

Since the pioneering work of Miller[2], it has been known that virtually every electrical measurement on semiconductors can be implemented by contactless inductive coupling, i.e. without the need for actual physical wire contact. We will be describing contactless radio frequency bridges which can measure d.c. conductivity and pulsed photoconductivity of semiconductors. Sophisticated contactless measurements, with no need for standard device processing, allow rapid monitoring of *minority* carrier properties such as: epitaxial heterostructure quality for different growth methods[3]; wafer substrate quality; interfacial recombination[4]; chemical synthesis of nearly ideal electronic[5–7] surfaces; radiative electron–hole recombination[8]; heterojunction bipolar transistors[9]; and rapid contactless evaluation of semiconductor process development[10]. Likewise, contactless measurements of *majority* carrier properties have been valuable for determining: sheet conductivity[11] of *p*-ZnSe layers for which ohmic contacts are unavailable; and band-bending[12] at semiconductor surfaces in darkness and light.

A block diagram of the inductively coupled radio frequency bridge, suited for Si work, operating at 70 MHz is shown in Fig. 1. A similar laser pumped apparatus, designed for the higher speeds of III–V semiconductors, operating at 500 MHz is shown in Fig. 2. This inductively coupled radio frequency apparatus monitors the absolute sheet conductivity of the semiconductor, both statically and pulsed.

The heart of the system is a 3–5 turn radio coil about 1 cm in diameter. In effect the coil is the primary of a transformer, and the semiconductor wafer is a one-turn secondary. The effective resistance in the secondary circuit will be boosted by the turns ratio squared when monitored in the primary circuit. If we approximate the secondary circuit resistance
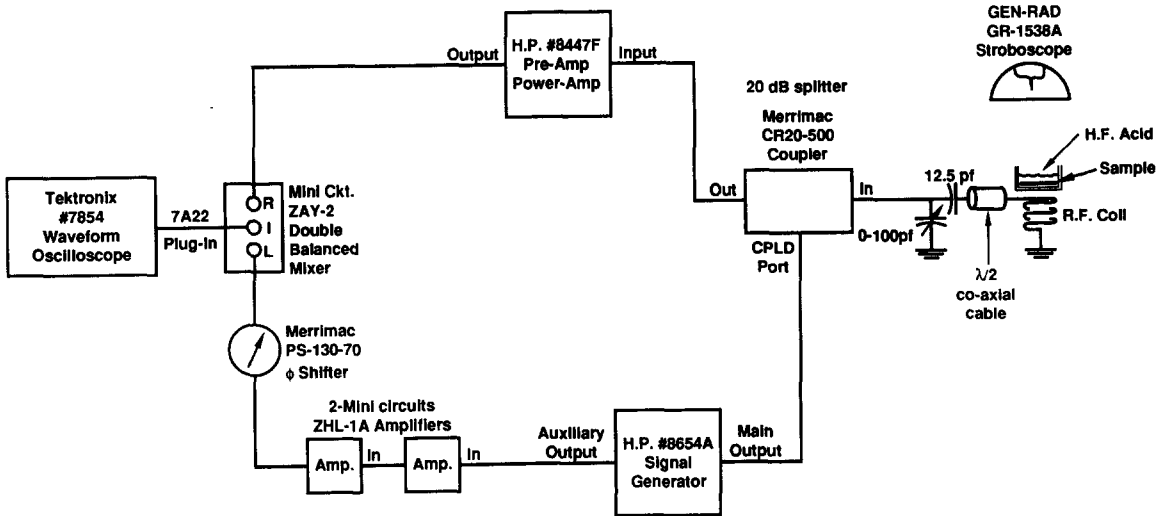
Fig. 1. A block diagram of an RF bridge operating at 70 MHz suited to minority carrier lifetime measurements on Si. A 20 dB splitter separates the incoming from the reflected signal. The imbalance in the circuit caused by the carriers is phase detected by a wide dynamic range double-balanced-mixer (DBM) and then digitized.

as being the sheet resistance of the semiconductor wafer, then a sheet resistance of $100\,\Omega\,\square^{-1}$ will look like $\sim 1000\,\Omega$ in parallel with the primary. The RF bridge is balanced when the primary circuit is forced to mimic a $50\,\Omega$ resistor by the fixed- and variable-tuning capacitor. Then there will be no reflection at the end of the $50\,\Omega$ coaxial cable leading to the primary. Small sheet conductivities in the semiconductor wafer will only perturb the tuning. The reflected RF wave from the primary coil will be linearly proportional to sheet conductivity of the semiconductor wafer. However if the sheet conductance change is as high as $\sim 0.2\,\Omega^{-1}\,\square$, it will look like $\sim 50\,\Omega$ in the primary and will exceed the linear dynamic range of the circuit.

The circuits are designed to digitize the reflected RF signal due to the impedance imbalance caused by the sheet conductivity changes in a semiconductor wafer. If known calibration wafers are repositioned to the exact same geometry, then the bridge signal can be calibrated absolutely in $\Omega^{-1}\,\square$. In effect we have a very fancy, inductively coupled, time resolved,
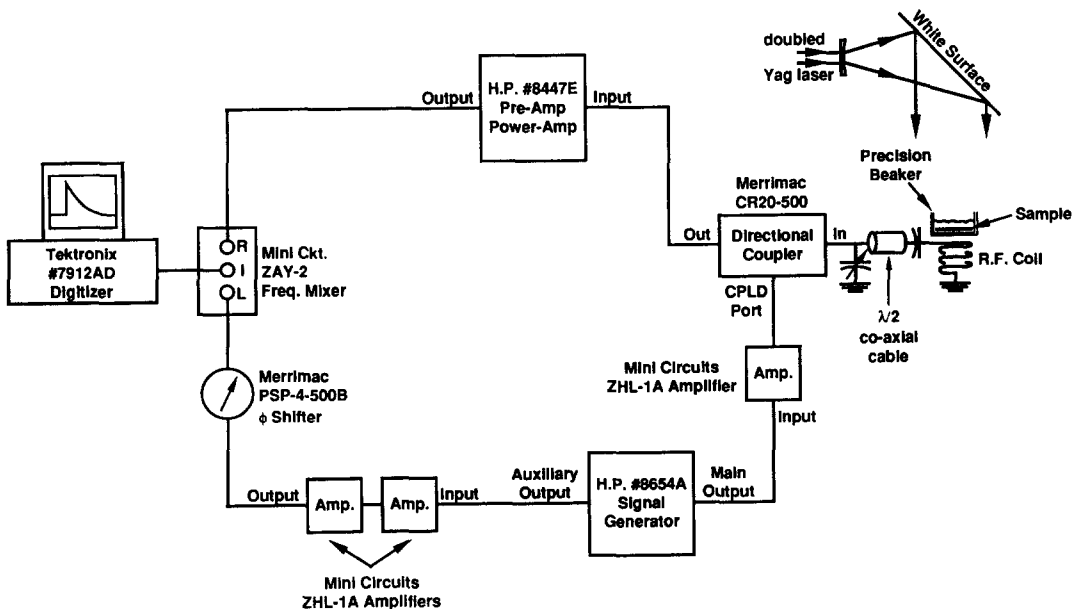
Fig. 2. An RF bridge operating at 500 MHz, fast enough to make lifetime measurements on III–V semiconductors. A doubled Nd:Yag laser scatters off a white surface and injects carriers into a GaAs double heterostructure epilayer.

ohmmeter. The actual circuits shown in Figs 1 and 2 were adapted from those radio circuits used in nuclear magnetic resonance[13].

When the RF bridge is operated in the photo-conductivity mode it can be a particularly valuable probe of minority carrier properties. A brief flash of pulsed incoherent light, from either a strobe lamp or a Q-switched doubled Nd:Yag laser (attenuated by scattering off a white surface), injects electrons and holes into an epilayer or into a bulk substrate wafer itself. The recombination of electrons with holes is monitored by the decay of the conductivity associated with the optically injected carriers. In a numerical algorithm, conductivity is divided by the carrier-density-dependent mobility to convert it to a density decay curve. If the epilayer thickness L is sufficiently small, the decay of excess carrier density n is simply the sum[14] of a bulk and a surface term:

$$\frac{dn}{dt} = -\left[\frac{1}{\tau_b} + \frac{2S}{L}\right]n, \qquad (1)$$

where τ_b is the bulk recombination lifetime, S is the surface recombination velocity and the factor 2 accounts for the front and back surfaces. The reciprocal of the quantity in brackets was called by Shockley[14] the "filament lifetime" τ, which in general may depend on n. Irrespective of the absorption depth of the light source, the injected carrier density n will become spatially uniform and eqn (1) will be valid provided that $L \ll \sqrt{D\tau}$ where D is the ambipolar diffusion constant and $\sqrt{D\tau}$ is the diffusion length. If the front and back surfaces of the epilayer

are inequivalent then $(S_f + S_b)$ should be substituted for $2S$.

In this paper we will review the operation of the contactless RF minority carrier lifetime bridge and show how it can be a real workhorse in the laboratory environment. The main advantage of this equipment is that it can give immediate answers about the semiconducting quality of unprocessed or partially processed materials. We will examine the utility of this type of apparatus by reviewing some of the applications where it was found useful.

EPITAXIAL QUALITY

The first application will be to compare[3] the quality of III–V double heterostructures which are grown by the three most common growth methods: organometallic chemical vapor deposition (OMCVD), liquid phase epitaxy (LPE) and molecular beam epitaxy (MBE). In making these comparisons, it is significant that the epitaxial layers are not subjected to any processing after growth. Because there are no contacts required, we detect the material quality directly as grown, without the degradation that might be caused by a high-temperature alloying step. The best and most consistent minority carrier properties came from OMCVD, but the other growth methods were almost as good. Figure 3 shows the decay of minority carrier density of one of the better OMCVD double heterostructures that we have tested. The initial decay at high densities is due to radiative and Auger recombination. The long
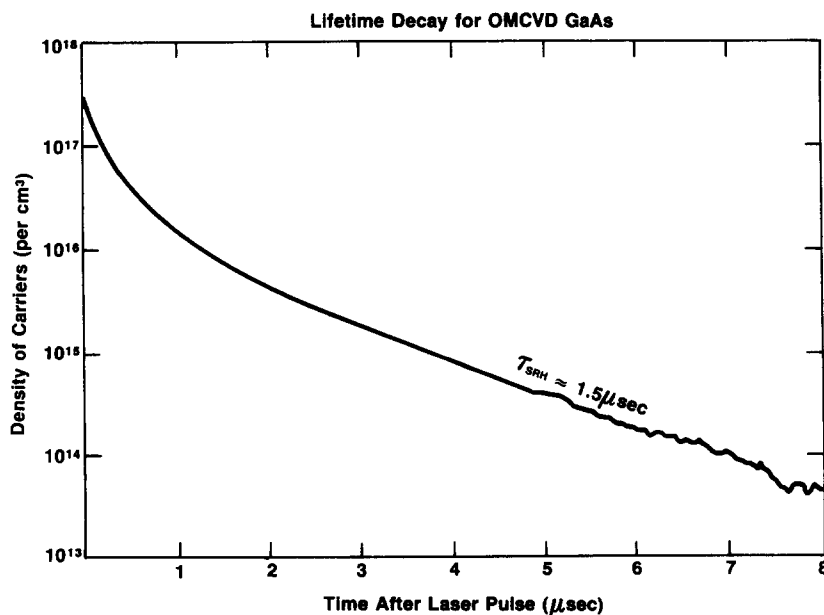

Fig. 3. The decay of carrier density in an OMCVD GaAs double heterostructure excited by delta function optical injection at $t = 0$. At long times and low densities bulk Shockley–Read–Hall recombination dominates all surface, radiative or Auger recombination and leads to an exponential decay lifetime $\sim 1.5\,\mu s$.

exponential tail at low density is due to Shockley–Read–Hall recombination which is defect sensitive. Typically τ_{SRH}, the Shockley–Read–Hall lifetime was 1–2 μs for OMCVD material, 0.5–1 μs for LPE material and 0.25–0.5 μs for MBE material.

These lifetimes are much longer than accepted by conventional wisdom, but they agree in line [15] with independent measurements. Conventional wisdom would have a III–V lifetime of only a few nanoseconds. This erroneous impression is based on: (i) heavily-doped (10^{18} cm^{-3}) or highly-injected material in which Auger and radiative recombination are fast; (ii) bare GaAs rather than double heterostructure material in which the surface recombination is prevented; and (iii) substrate grade material which is poor, rather than epitaxially grown material which is excellent.

The bulk Shockley–Read–Hall lifetime is often expressed as $1/\tau_{SHR} = N_t v_{th} \sigma$. Typical values of the carrier thermal velocity are $v_{th} \approx 10^7$ cm s^{-1} and for the capture cross-section $\sigma \sim 10^{-15}$ cm^2. Then the deep recombination center density N_t would be approx. 10^{14} defects cm^{-3} which is a reasonable deep trap concentration for our high-quality material. A possible objection to this interpretation of our rather long measured lifetimes is that they may have been increased by the ratio of time spent in traps to the time spent as free electrons. In many "dirty" photoconductors[16], the shallow trap density is higher than the injection level and the carriers become stored in shallow traps where they neither recombine nor contribute to the conductivity. Then the lifetime is increased by the ratio of the number of trapped electrons to the number of free electrons. There are two reasons why this is not happening here: (1) if a significant fraction, say 10%, of the injected electrons were in traps, they could not contribute to the photoconductivity and would present a 10% error in the absolute signal level, which would easily have been detected; and (2) the excellent bulk quality ensured that all traps would be saturated at injection levels above 10^{15} cm^{-3}. It may be worth noting the Nelson's photoluminescence decay lifetime experiment{15}, which does not lend itself so readily to absolute calibration, could not rule out the possibility of a shallow trap-dominated lifetime.

The long lifetimes measured here show that GaAs material quality need not be a limitation to the performance of minority carrier electronic devices. In practice, however, considerable deterioration arises during device processing and it would be valuable to repeat this type of measurement at each processing step to identify the lifetime killing steps. That will be discussed later in the paper.

SURFACE QUALITY

The second application we will discuss is the exploration for surface chemical treatments[6] which produce a surface recombination velocity (SRV)
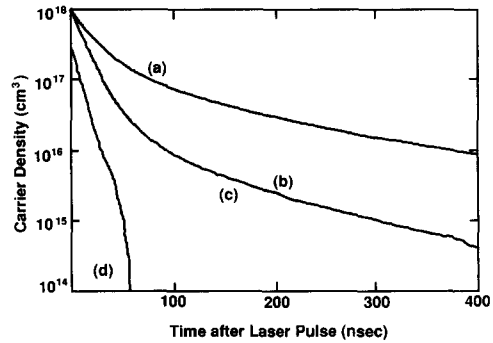

Fig. 4. The carrier density decay in a GaAs double heterostructure excited by delta function optical injection at $t = 0$ for four different surface treatments: (a) AlGaAs/GaAs; (b) As$_3$S$_2$/GaAs/AlGaAs double heterostructure before aging; (c) the same surface after 4 months aging on the shelf; and (d) clean GaAs surface exposed to air.

which begins to compete, for example, with the excellent AlGaAs/GaAs interface. The minority carrier lifetime bridge is a superb exploratory tool since different chemical preparations can be tried one after the other with no special device fabrication in between. A "cut and try" approach makes sense if we can try many different chemical reagents in a brief time. Then we can quickly converge on a good chemical process by trying many different variations on any particular approach that appears promising.

The best surface chemical treatments so far: for GaAs, an amorphous film[6] of As$_3$S$_2$; for In$_{0.53}$Ga$_{0.47}$As, a polycrystalline film [7] of NaOH; for Si, a treatment in [5] HF acid. The respective carrier density decay curves are shown in Figs 4–6. Figure 4 compares the density decay in a GaAs double heterostructure excited by delta function optical injection at $t = 0$ for four different surface treatments: (a) AlGaAs/GaAs; (b) As$_3$S$_2$/GaAs/AlGaAs double heterostructure before aging; (c) the same surface after 4 months aging on the shelf; and (d) clean
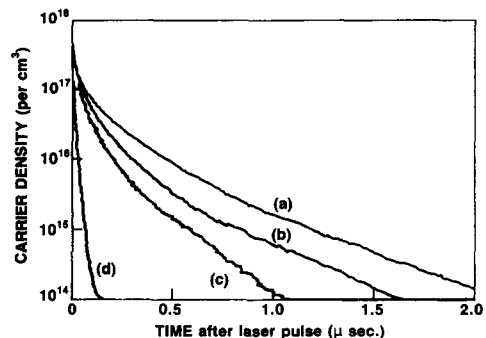

Fig. 5. The decay of carrier density in an InP/In$_{0.53}$Ga$_{0.47}$/As/InP double heterostructure excited by delta function optical injection at $t = 0°$: (a) the intact InP/In$_{0.53}$Ga$_{0.47}$As/InP double heterostructure; (b) aqueous 10 M NaOH/In$_{0.53}$Ga$_{0.47}$Ga$_{0.47}$As after 30 min at $T = 20°$C; (c) spun dry NaOH/In$_{0.53}$Ga$_{0.47}$As; and (d) native oxide/In$_{0.53}$Ga$_{0.47}$As.
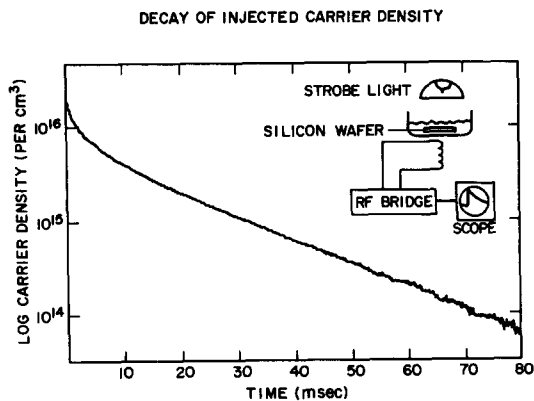
DECAY OF INJECTED CARRIER DENSITY

Fig. 6. Semilog plot of the carrier density decay from a particularly long-lived $250\,\mu$m thick Si $\langle 111 \rangle$ sample immersed in HF acid.

Fig. 7. When the deay rate at a given injection level is plotted against reciprocal thickness, the surface and bulk contributions can be distinguished as shown.

GaAs surface exposed to air. The As_3S_2/GaAs surface has led to high-gain heterojunction bipolar transistors[9] in which the current gain was increased by over an order of magnitude. As was well known from the first bipolar transistors[14], they are acutely sensitive to surface quality.

Figure 5 compares four different surface treatments on $In_{0.53}Ga_{0.47}As$ excited by delta function optical injection at $t = 0$: (a) the intact $InP/In_{0.53}Ga_{0.47}As/InP$ double heterostructure; (b) aqueous 10 M NaOH/$In_{0.53}Ga_{0.47}As$ after 30 min at $T = 20°C$; (c) spun-dry NaOH/$In_{0.53}Ga_{0.47}As$; and (d) native oxide/$In_{0.53}Ga_{0.47}As$. It should be remarked that the surface quality of $In_{0.53}Ga_{0.47}As$ before special chemical treatment is superior to a GaAs surface which enjoys a sulfide coating. The remarkably favorable surface quality of $In_{0.53}Ga_{0.47}As$ lends itself to the formation[7] of "naked quantum wells" in which one face of the quantum well is exposed.

Figure 6 shows the carrier density decay from a particularly long lived sample of float-zone Si which had been chemically oxidized and then tested in hydrofluoric acid. The time scale is tens of milliseconds rather than the microseconds or less as for the III–V semiconductors. The difference is not simply due to the contrast between direct and indirect gap materials. In fact the quality of the best float-zone Si is 10^4 better than the best III–V expitaxial material. This can be translated into the number of Shockley–Read–Hall defects cm^{-3}. Where previously we discussed 10^{14} defects cm^{-3} for GaAs, we must now speak of 10^{10} defects cm^{-3} for selected float-zone Si. Since the HF treatment is so easy, it is straightforward to survey many different batches of Si to find the better ones.

Such a good bulk lifetime can only be monitored in the presence of an excellent SRV. The surface quality can be separated out by comparing different thicknesses as the same sample is etched down. This is shown in Fig. 7. The slope gives the SRV
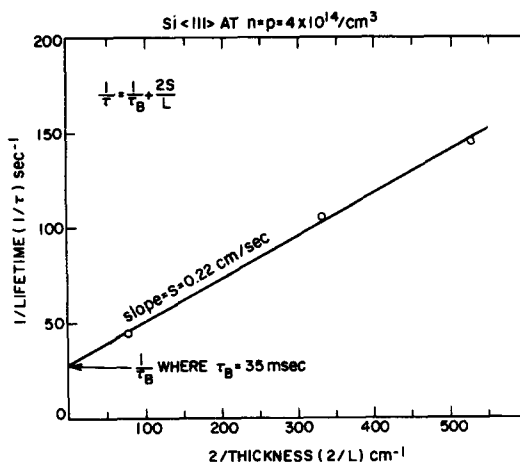
which was around $0.25\,cm\,s^{-1}$ for Si $\langle 111 \rangle$. A summary of everything we have learned about SRV in the major semiconductors is graphically illustrated in Fig. 8. When the surface is at its worst possible, SRV $\sim 10^7\,cm\,s^{-1}$ in all cases. The best SRV of any semiconductor interface is HF treated Si $\langle 111 \rangle$. All the other surface treatments fall somewhere in between. Indeed, by raising the pH of the hydrofluoric acid, Higashi et al.[17] were able to obtain a surface that was both atomically flat as well as having the lowest known SRV.
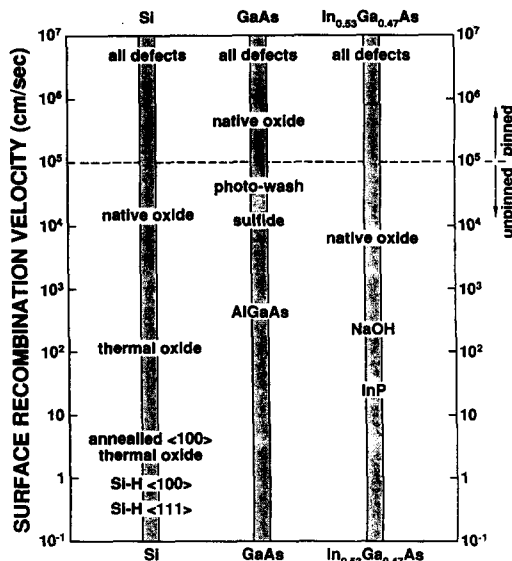

Fig. 8. A summary of everything we have learned about chemically prepared semiconductor surfaces, covering a dynamic range of 8 decades of SRV. InP and AlGaAs are of course lattice-matched heterostructures. The Si–H surface is measured under acid. "All defects" refers to the worst possible case of virtually every surface bond being defective. Pinned and unpinned is only a qualitive distinction, which occurs around SRV $\sim 10^5\,cm^{-1}$ s.

BULK WAFER QUALITY

One byproduct of the capability to create a nearly ideal semiconductor surface chemically is that it eliminates surface recombination permitting us to focus on bulk quality. Therefore we have looked at the bulk minority carrier lifetime of substrate wafers whose surfaces had been chemically treated to effectively eliminate surface recombination. The conclusion is that bulk III–V wafer material never seems to have a lifetime longer than 10 or 20 ns, while epitaxial material grown on those wafers can be as much as 100 times better. Similarly we surveyed bulk Si wafers and found that commercial float-zone Si is sometimes as good as 35 ms, as shown in Fig. 7, but that Czochralski material is generally about 1000 times worse.

We should emphasize that these measurements are taken on essentially unprocessed wafer material. The results could be worse as a result of thermal processing. This suggests the use of the lifetime bridge as a process monitor. Since it requires no special wafer processing itself, contactless lifetime monitoring is excellent for before/after tests. We have used it to make seemingly minor, but critical adjustments in Si oxidation conditions[4] to sustain minority carrier lifetime in oxidized float-zone material. Likewise, we have used it to perfect the process conditions[10] for minimizing the forward leakage current of SIPOS heterojunction contacts on Si.

DOPING LEVELS IN p-ZnSe

Normally ZnSe is available as an n-type semiconductor. For many years there has been speculation that p-type dopants in ZnSe are inherently self-compensating, and that therefore p-type conductivity would be impossible to achieve. That point of view has now been overturned in the most direct way possible, by an existence proof. Using an activated form of nitrogen, from a free radical dopant source, ZnSe has now been grown to be p-type. The importance of this development cannot be overestimated. It will extend GaAs opto-electronic technology to those blue and green wavelengths which have thus far been inaccessible to good-quality double heterostructures. Since ZnSe is grown on GaAs, to which it is nearly lattice-matched, these II–VI's will be a major boost to III–V opto-electronic technology as well.

Thus far the p-doping levels are only in the mid-10^{17} cm^{-3} range, much higher than earlier hoped, but about an order of magnitude lower than required for ohmic contacts. This has been an impediment to progress. Without a rapid means of determining doping levels, the feedback to the crystal growers is very slow. Since the optimization of doping conditions requires trial and error during many growth runs, fast feedback of information to the crystal grower permits him to vary growth conditions so as to converge on the most effective p-type doping conditions.

Once again the contactless inductively coupled conductivity bridge can play a role. It can reveal the p-type conductivity levels, even though the doping is insufficient to permit ohmic contacts. In this manner growth conditions were defined[11] which produce a p-type conductivity of 0.75 Ω-cm. Assuming the hole mobility to be in the range 10–20 cm^2 V^{-1} s^{-1}, this implies a free hole density of 4×10^{17}–8×10^{17} cm^{-3}. Given the importance of this material breakthrough, further intensive work should generate the needed improvements in material quality and doping levels.

BAND BENDING AT SEMICONDUCTOR SURFACES

Mostly in this article we have focused on minority carrier properties. But doping levels, as discussed in the previous section, are a majority carrier property. Lifetime measurements are not needed, it is enough to simply measure the majority carrier conductivity, albeit by a contactless technique. Within a depletion length, surface charge leads to band bending[12] and similar effects. The loss of majority carriers near a surface causes a drop in the observed sheet conductivity of a doped layer.

In effect, the inductively coupled RF bridge is a type of field effect transistor. Since the current loops are driven by magnetic induction, no source or drain are needed. Furthermore since the field effect is determined by surface charges which are controlled chemically, no gate electrode is needed. We are in the interesting position of doing field effect transistor measurements, but there is no source, no drain and no gate!

Perhaps the most interesting part of the measurement is the effect of low light levels on the bandbending of a semiconductor such as GaAs. The quasi-Fermi level separation induced by weak light flattens the bands near the surface. In fact the voltage change at the surface depends logarithmically on the light intensity, so small light levels can have surprisingly large effects. The equation for this surface photovoltage is essentially similar to the formula for solar cell output voltage which is proportional to the same logarithm of light intensity. This effect should not be overlooked in the course of measuring minority carrier lifetimes. The first effect of incident light is to change the majority carrier concentration near surfaces. As the light intensity goes up, eventually there is a crossover where the increased number of minority carriers finally contributes more to the electrical conductivity than the majority carriers in the depletion layer.

At low injection levels there will be a conductivity decay which is very slow and which is due to slow changes in majority carrier depletion near surfaces. This may take seconds and should not be confused with minority carrier recombination lifetimes which are always much faster. Upon examining a transient

photoconductivity decay curve, there will be a slowly decaying pedestal upon which the faster minority carrier decay is superimposed. The two effects can usually be separated since their timescales are so very different. Another distinction is that the minority carrier signal is coming from the bulk and its conductivity is proportional to thickness. The surface depletion gives an unchanged signal as long as the sample is thicker than two depletion lengths. In Ref. [12], the changes in surface band-bending caused by surface chemical treatments were measured. Furthermore the band-flattening effect of low light levels was shown to be well-modeled by a solar cell equation.

We have sought to show that contactless minority carrier lifetime measurement with the photo-pumped RF bridge can be an indispensable tool in any semiconductor laboratory. In conjunction with some of the chemical surface treatments its analytical capabilities extend over a broad range of processed and unprocessed semiconductors.

REFERENCES

1. E. Yablonovitch and T. J. Gmitter, *Proc. Symp. on Diagnostic Techniques for Semiconductor Materials and Devices* (T. J. Shaffner and D. K. Schroeder, Eds), Vols 88–20, pp. 207–218. The Elechem. Soc., Pennington, NJ (1988).
2. G. L. Miller, D. A. H. Robinson and S. D. Ferris, *Proc. Elechem. Soc.* **78**, 1 (1978).
3. E. Yablonovitch, R. Bhat, J. P. Harbison and R. A. Logan, *Appl. Phys. Lett.* **50**, 1197 (1987).
4. E. Yablonovitch, R. M. Swanson, W. D. Eades and B. R. Weinberger, *Appl. Phys. Lett.* **48**, 245 (1986).
5. E. Yablonovitch, D. L. Allara, C. C. Chang, T. Gmitter and T. B. Bright, *Phys. Rev. Lett.* **57**, 249 (1986).
6. E. Yablonovitch, C. J. Sandroff, R. Bhat and T. Gmitter, *Appl. Phys. Lett.* **51**, 439 (1987). Also: E. Yablonovitch, T. J. Gmitter and B. G. Bagley, *Appl. Phys. Lett.* **57**, 2241 (1990).
7. E. Yablonovitch, H. M. Cox and T. J. Gmitter, *App. Phys. Lett.* **52**, 1002 (1988).
8. E. Yablonovitch, T. J. Gmitter and R. J. Bhat, *Phys. Rev. Lett.* **61**, 2546 (1988).
9. C. J. Sandroff, R. N. Nottenburg, J.-C. Bischoff and R. Bhat, *Appl. Phys. Lett.* **51**, 33 (1987). Also: H. L. Chung, M. S. Carpenter, M. R. Melloch, M. S. Lundstrom, E. Yablonovitch and T. J. Gmitter, *Appl. Phys. Lett.* **57**, 2113 (1990).
10. E. Yablonovitch and T. Gmitter, *IEEE Electron Device Lett.* **EDL-6**, 597 (1985).
11. R. M. Park, M. B. Troffer, E. Yablonovitch and T. J. Gmitter, *Appl. Phys. Lett.* **59**, 1896 (1991).
12. E. Yablonovitch, B. J. Skromme, R. Bhat, J. P. Harbison and T. J. Gmitter, *Appl. Phys. Lett.* **54**, 555 (1989).
13. E. Fukushima and S. B. W. Roeder, *Experimental Pulse NMR, A Nuts and Bolts Approach*, pp. 394 and 414. Addison-Welsey, Reading, MA (1981).
14. W. Shockley, *Electrons and Holes in Semiconductors*, p. 318. Van Nostrand, New York (1950).
15. R. J. Nelson and R. G. Sobers, *J. appl. Phys.* **49**, 6103 (1978). Also: G. W.'t Hooft, C. V. Opdorp, H. Veenvliet and A. T. Vink, *J. Cryst. Growth* **55**, 173 (1981).
16. A. Rose, *Concepts in Photoconductivity and Allied Problems*. Krieger, Huntington, NY (1978).
17. G. S. Higashi, Y. J. Chabal, G. W. Trucks and K. Ragavachari, *Appl. Phys. Lett.* **56**, 656 (1990).